Analytical and Bioanalytical Chemistry
https://doi.org/10.1007/s00216-020-02440-y

RESEARCH PAPER

A visual electrochemiluminescence biosensor based on CuInZnS quantum dots for superoxide dismutase detection

Yang Liu [1,2] · Kunliang Jiang [1,2] · Yixin Nie [1,2] · Yupeng Guo [1,2] · Qiang Ma [1,2]

Received: 6 November 2019 / Revised: 10 January 2020 / Accepted: 17 January 2020

Abstract

Superoxide dismutase (SOD), also known as liver protein, is a substance widely distributed in various biological cells. It has the function of catalyzing the disproportionation reaction of superoxide free radicals. SOD can form an antioxidant chain together with peroxidase, catalase, and other substances in the body of organisms, and thus, is one of the indispensable important substances in the body of organisms. In this work, we provided a simple and fast visual electrochemiluminescence (ECL) sensor for SOD detection. CuInZnS quantum dots (QDs) worked as the ECL luminophore with hydrogen peroxide as co-reactant. In the sensing process, SOD and CuInZnS QDs on a glassy carbon electrode (GCE) competed with each other for hydrogen peroxide to produce superoxide during electrochemical luminescence, thus quenching the ECL signal of CuInZnS QDs. The proposed sensor can quantify SOD with a limit of detection (LOD) of 0.03 μg/mL. In addition, the change in the CuInZnS QDs ECL signal was easily observed with a smartphone camera. The results indicated that this sensor could effectively work in the detection of SOD in human blood.

Keywords Superoxide detection · Visual ECL detection · CuInZnS QDs

Introduction

Superoxide dismutase (SOD) is an antioxidant widely distributed in various biological cells. The activity of SOD was first discovered by Irwin Fridovich and Joe M. McCord. In the following years, the antioxidant capacity of SOD was widely studied. And antioxidant capacity of SOD was applied in the fields of clinical diagnosis and treatment, food, cosmetics, animal feeding, plant cultivation, and other fields. The main function of SOD is to catalyze the disproportionation of superoxide, which is produced by biological cells in the process of metabolism to produce water and hydrogen peroxide [1, 2]. SOD can catalyze the dismutation reaction of superoxide to generate hydrogen peroxide which is harmful to human body, then catalase (CAT) and peroxidase (POD) catalyze the decomposition of hydrogen peroxide to eventually generate water and oxygen. SOD, POD, and CAT constitute a complete chain of antioxidant in organisms and play an extremely important role in organisms. Because SOD plays an extremely important role in human body, real-time quantitative detection of sod content in human tissues has important clinical significance. For example, it is used in patients with free radical metabolic disorder to judge the clear intervention measures of free radicals and the damage of free radicals. The overexpression of SOD2 is found in cancerous cells of breast cancer, pancreatic cancer, papilloma, prostate cancer, and other cancers, and trisomy 21 syndrome is closely related to the overexpression of SOD1 [3–5]. Therefore, some detection methods have been developed for SOD, including enzyme-linked immunosorbent assay (ELISA), chemiluminescence detection, and electrochemical detection. Although these methods exhibit high sensitivity and analysis precision, complex detection process and expensive cost is still required. Therefore, the development of a convenient and rapid method for the detection of SOD is still essential.

Electrochemiluminescence (ECL), combines the characters of electrochemistry and luminescence, has the advantages of

Electronic supplementary material The online version of this article (https://doi.org/10.1007/s00216-020-02440-y) contains supplementary material, which is available to authorized users.

✉ Qiang Ma
Qma@jlu.edu.cn

[1] Department of Analytical Chemistry, College of Chemistry, Jilin University, Changchun 130012, Jilin, China

[2] National Chemistry Experimental Teaching Demonstration Center, Jilin University, Changchun 130012, Jilin, China

Published online: 03 February 2020

simple instrument and high sensitivity [6–8]. ECL is the phenomenon of light radiation caused by the energy relaxation of the excited species triggered by electrochemistry [9, 10]. The ECL mechanism can be divided into two types, the annihilation ECL and the co-reactant ECL. Annihilation pathway refers that the system can accept and give electrons respectively, and then under the external electric field, the electrode surface generates a pair of reversible anionic and cationic radicals through disproportionation reaction [11]. The two radicals then undergo a radical annihilation reaction, which produces an excited state of the material with ECL signal. In the co-reaction ECL reaction, the intermediate transition state with strong redox ability can be generated through electrochemical oxidation (or reduction) [12]. The transition state can react with ECL luminescent body which is oxidized (or reduced) by electrochemical oxidation (or reduction) to obtain the luminescent excited state. Common co-reaction agents include persulfate and hydrogen peroxide. Semiconductor nanocrystals or quantum dots (QDs), as a new kind of ECL nanocrystals, have been developed and attracted great interest of researchers. The ECL phenomenon of Si QDs in organic systems was first reported in 2002 [13]. Until now, many ECL sensors were developed based on QDs and other nanomaterials [14]. Compared with traditional molecular luminescence such as Ru $(bpy)_3^{2+}$, QDs has its unique advantages, such as more controllable surface defects, size effect of luminescence and good light tolerance, and milder luminescence system. Although many QDs have been applied as ECL luminophore, such as CdTe QDs [15], CdTe@ZnS QDs [16], and CdSe QDs [17], the important limitation of QD-based ECL applications is the toxicity from heavy metal elements. Therefore, the heavy metal free semiconductor QDs have employed to solve the toxicity of QDs. In recent years, quaternary non-toxic CuInZnS QDs have been widely used in sensor construction [18–21]. The quaternary CuInZnS QDs exhibited good thermal stability. There are two main synthesis methods of CuInZnS QDs, one is hydrothermal synthesis method and the other is metal-organic synthesis method. Metal-organic phase synthesis of CuInZnS QDs takes place in an organic solvent and is accompanied by high synthesis temperatures. The synthesis process usually has high production costs. Therefore, in order to have a better biological application prospect, hydrothermal synthesis method is usually used to synthesize CuInZnS QDs with low toxicity and good biocompatibility.

In this work, biocompatible CuInZnS QDs were prepared as ECL luminescent and hydrogen peroxide (H_2O_2) as co-reactant. SOD can compete with CuInZnS QDs for superoxide, which produced by H_2O_2 reduction process (Scheme 1). As a result, with the concentration of SOD increasing, the ECL signal of CuInZnS QDs decreased gradually. Furthermore, the ECL signal changes of CuInZnS QDs were clearly recorded by the smartphone CMOS camera. The ECL visual detection was of great significance in clinical medicine. Visual detection required sensitive, convenient, and fast detection equipment. In the process of detection, visual detection was timely and the results were intuitive and clear. Compared with the fluorescence signal, the ECL signal was weak and not easy to be captured. So the realization of ECL visualization became very important. Therefore, we designed software to analyze the thermal diagram of the light intensity distribution. The prepared sensor was applied to the rapid detection of SOD in human blood with high selectivity and high sensitivity.

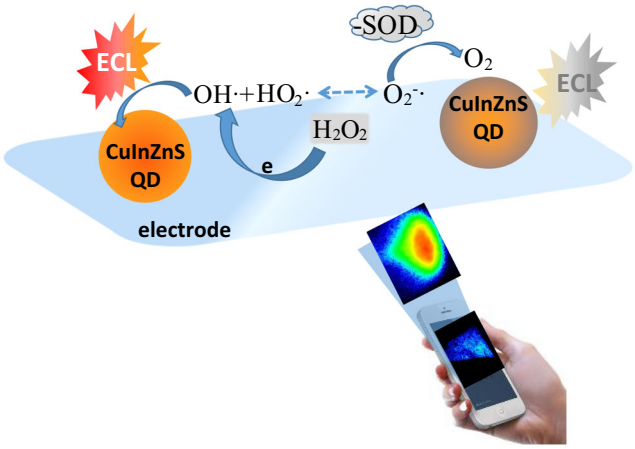

Scheme 1 The schematic illustration of the ECL sensor for determination of SOD

Experiment section

Materials

Copper(II) chloride dehydrate ($CuCl_2{\cdot}2H_2O$, 99.0%), indium chloride hydrate ($InCl_3{\cdot}4H_2O$, 99.0%), zinc chloride ($ZnCl_2$, 98%), sodium hydroxide (NaOH, 96.0%), mercaptopropionic acid (MPA, 99.0%), thiourea ($CS(NH_2)_2$, 99.0%), and ethanol (C_2H_5OH, 99.7%) were purchased from Sigma Co. (Shanghai, China). SOD, hydrogen peroxide (30%), sodium dihydrogen phosphate (NaH_2PO_4), disodium hydrogen phosphate (Na_2HPO_4), sodium phosphate (Na_3PO_4), horseradish peroxidase (HRP), alkaline phosphatase (ALP), ALA (alanine), ARG (arginine), THR (threonine), GLY (glycine), VAL (valine), LYS (lysine), and GSH (glutathione) were obtained from Sinopharm Chemical Reagent Co. Ltd. Human serum samples were obtained from the China-Japan Union Hospital of Jilin University.

Apparatus

TEM images of the QDs were obtained with a Hitachi electron microscope operating at 200 kV acceleration voltages. FTIR was obtained from Thermo Nicolet 360 FTIR spectrometer.

Photoluminescence (PL) and UV–vis absorption spectra were acquired by Shimadzu RF-5301 PC spectrofluorophotometer and Hitachi UH5300 UV–vis spectrometer, respectively. The CV and EIS data were acquired with a CHI 660B electrochemical workstation with the glassy carbon electrode (GCE) as the working electrode. In the all electrochemical analysis process, a platinum wire and an Ag/AgCl (saturated KCl) electrode was employed as the counter electrode and the reference electrode, respectively.

Synthesis of CuInZnS QDs

CuInZnS QDs were synthesized by hydrothermal method. $CuCl_2{\cdot}2H_2O$, $InCl_3{\cdot}4H_2O$, and $ZnCl_2$ solutions were added to conical flask, respectively. The molar ratios of $CuCl_2{\cdot}2H_2O$, $InCl_3{\cdot}4H_2O$, and $ZnCl_2$ are 3:10:5. Then distilled water and MPA solution were added to conical flask, the solution became turbid to produce yellow particles. The pH value of the solution was adjusted to 11.3 by adding 4 mol/L NaOH with stirring for 10 min. $CS(NH_2)_2$ solid was added to the system, and the solution appeared pale pink after dissolving. The above mixture was transferred into Teflon-lined stainless-steel autoclave. And the autoclave was placed in the oven at 180 °C for 5 h. The quantum yield of the CuInZnS QDs samples was measured according to the reported quantum yield of Rhodamine 6G. And the QY of CuInZnS QDs was 6%.

ECL and visual detection

The bare glassy carbon electrode (GCE) was polished with 1.0 and 0.05 μm α-Al_2O_3 powder. The GCE was ultrasonic in ethanol and water respectively. The cleaned GCE was soaked in poly dimethyl diallyl ammonium chloride (PDDA) solution for 5 min and dried under N_2 atmosphere. Then, 6 μL CuInZnS QDs was dropped on the PDDA/GCE film. For the measure of SOD, the obtained CuInZnS QDs/ PDDA/GCE film was immersed in 0.1 mol/L phosphate buffer solution (pH = 7.4) containing 30 mmol/L H_2O_2 as co-reactant and different concentration of SOD. The ECL signal was recorded in co-reactant under cyclic voltammetry from 0 to − 2.5 V.

For the visual detection, a 6 cm × 5 cm FTO glass was used as a working electrode. And the construction of the system

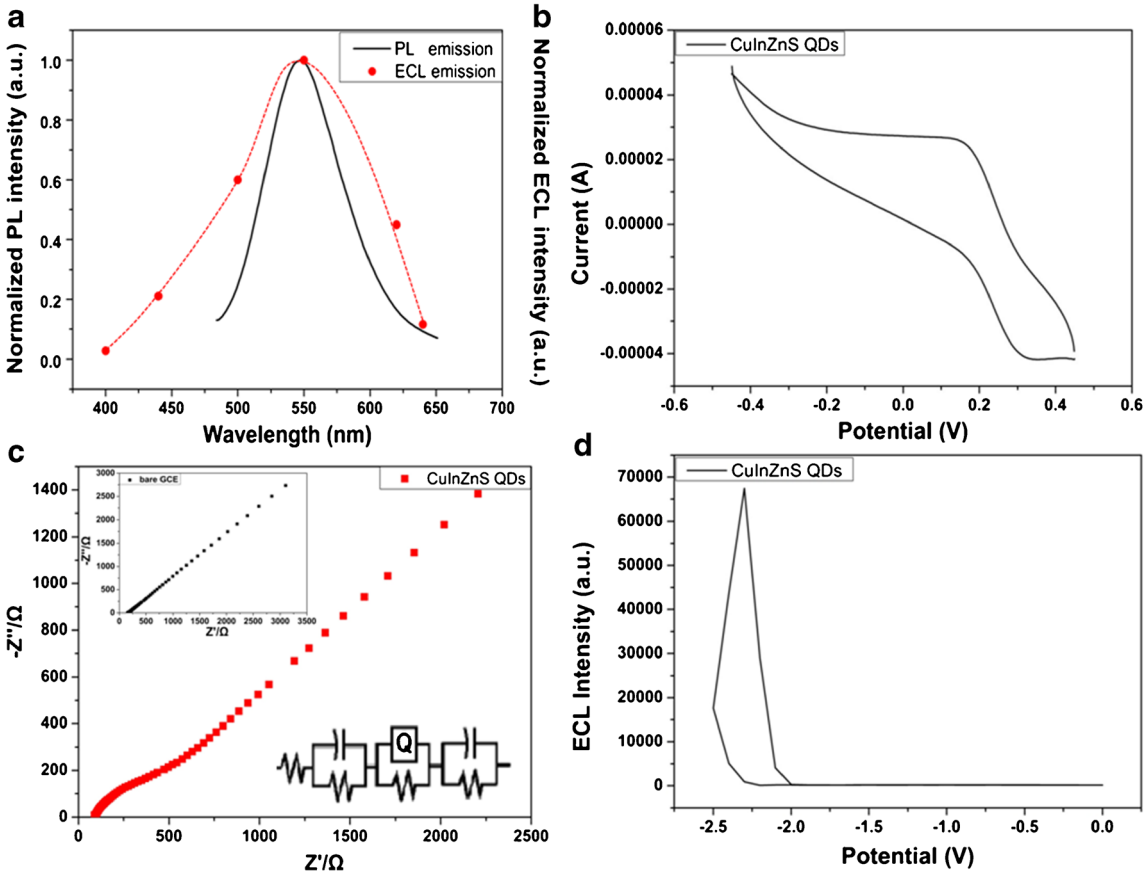

Fig. 1 **a** The PL and ECL emission spectrum of CuInZnS QDs. **b** The cyclic voltammograms of CuInZnS QDs in 0.1 mol L^{-1} KCl solution containing 1.0 mmol L^{-1} $K_3[Fe(CN)_6]/K_4[Fe(CN)_6]$. **c** The EIS spectrum of CuInZnS QDs in 0.1 mol L^{-1} KCl solution containing 2.5 mmol L^{-1} $K_3[Fe(CN)_6]/K_4[Fe(CN)_6]$. The impedance spectra were recorded in the frequency range of 0.01 Hz–100 kHz with amplitude of 5 mV (Inset Fig: the EIS spectrum of bare GCE and the equivalent circuit diagram). **d** The ECL behavior of the CuInZnS QDs (Excitation voltage range from 0 V to − 2.5 V)

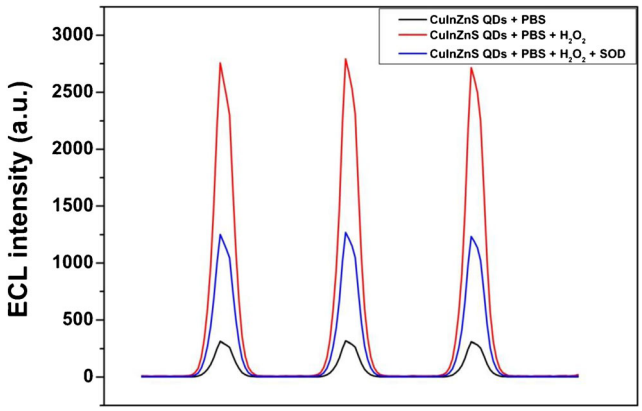

Fig. 2 The ECL curves of CuInZnS QDs in 0.1 mol/L phosphoric acid buffer (black curve), CuInZnS QDs in 0.1 mol/L phosphoric acid buffer containing 30 mmol/L H_2O_2 (red curve). 0.5 μg/L SOD CuInZnS QDs in 0.1 mol/L phosphoric acid buffer containing 30 mmol/L H_2O_2 (blue curve)

and the excitation potential was the same as the above ECL detection. In order to get the ECL images, an iPhone 7 smartphone with a CMOS camera chip (3174 × 2750 pixels, pixel size = 1.8 μm) was employed. The ECL image was smoothed with gaussian to remove noise. Then the gray value of each pixel was calculated. According to the obtained gray value, the pixel point was mapped by function f to a segment of color that changes continuously from black to red.

Results and discussion

Characterization of CuInZnS QDs

As shown in Fig. S1 (see Electronic Supplementary Material, ESM), the obtained CuInZnS QDs had uniform particle size distribution with average diameter of 6 nm. As shown in ESM Fig. S2 (A), the absorption peak of CuInZnS QDs was 418 nm. This was due to n-π* transition of C=O. And FTIR spectra confirmed the high occupation of oxygen-rich groups (ESM Fig. S2 (B)). The peaks at 1574 cm^{-1} and 1424 cm^{-1} were assigned to the asymmetric stretching vibration and symmetric stretching vibration of C=O, respectively. And the wide peak at 3400 cm^{-1} was due to the stretching vibration of O–H. The peaks at 2958 cm^{-1} and 2903 cm^{-1} were attributed to the asymmetric stretching vibration and symmetric stretching vibration of $–CH_2$, respectively. There was no characteristic peak of -SH of MPA at 2550–2680 cm^{-1}, which was due to the covalent bonds between -SH and metal atoms of the QDs. X-ray diffraction (XRD) was employed to identify the crystal structure of CuInZnS QDs. (ESM Fig. S3) Three characteristic peaks at 27.2°, 62.3°, and 77.2° corresponded to the (1 1 1), (2 2 0), and (3 1 1), which revealed that CuInZnS QDs was zinc blende type crystal.

ECL behavior of CuInZnS QDs

Figure 1a shows the PL and ECL emission spectrum of CuInZnS QDs. The PL emission peak was 548 nm and the ECL emission peak was 550 nm. The PL and ECL spectrum of CuInZnS QDs had a relatively large overlap. Different with the PL process, the electron transfer occurred on the surface of CuInZnS QDs in ECL reactions [21]. The ECL process occurred when two oppositely charged QDs collide. The electrons or holes tunnel through the ligands from one QD to the other and thus were affected by the ligands and QD surfaces [22, 23]. In the absence of a deep surface trap state, the injected electron or hole may relax in the core or surface state, at which point the ECL spectrum is expected to overlap with PL.

The mechanism for the process of radical annihilation ECL generation is according to the equations below:

$$QD - e^- \rightarrow QD^+ \quad (1)$$

$$QD + e^- \rightarrow QD^- \quad (2)$$

$$QD^+ \cdot + QD^- \cdot \rightarrow QD^* + QD \quad (3)$$

As shown in Fig. 1b, cyclic voltammetry (CV) was performed with a supporting electrolyte of 0.1 mol L^{-1} KCl and 1.0 mmol L^{-1} $K_3[Fe(CN)_6]/K_4[Fe(CN)_6]$. There was an oxidation peak at 0.178 V and a reduction peak at 0.315 V. It was

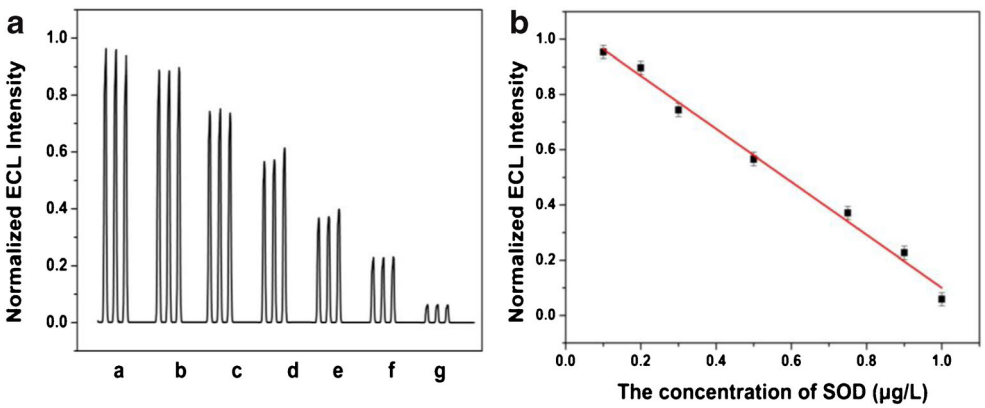

Fig. 3 **a** ECL traces of different concentrations of SOD in pH 7.4 0.1 mol/L phosphoric acid buffer containing 30 mmol L^{-1} H_2O_2 (from left to right: 0.1, 0.2, 0.3, 0.5, 0.75, 0.9, 1.0 μg/L). **b** Calibration curve for quantification of SOD

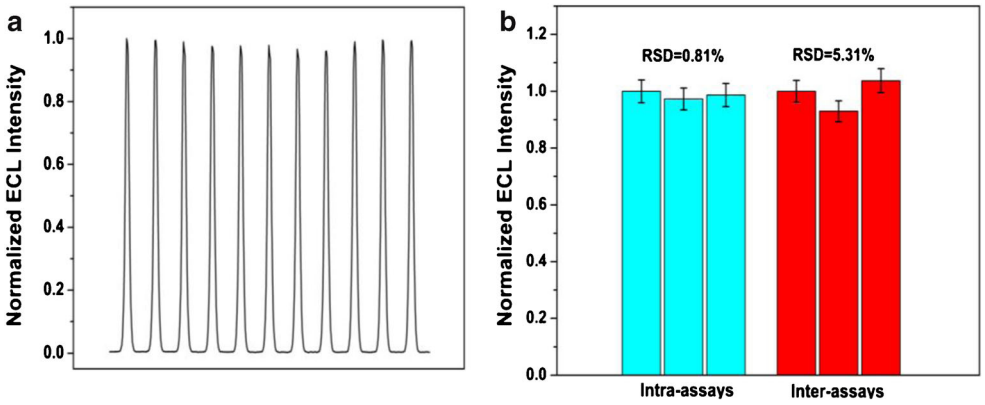

Fig. 4 **a** The stability and **b** reproducibility of the sensor (0.5 μg/L SOD/CuInZnS QDs in pH 7.4 0.1 mol/L phosphoric acid buffer containing 30 mmol L^{-1} H_2O_2)

due to the oxidation groups (–COOH) and reductive groups (–OH) on the surface of CuInZnS QDs. The electrochemical impedance spectroscopy (EIS) result was in Fig. 1c. The electron-transfer resistance of CuInZnS QDs was 201 Ω. The cleaned GCE showed a mass diffusion limiting process in the insert figure of Fig. 1c. The excitation potential was − 2.3 V (Fig. 1d).

Condition optimization

To achieve the ideal ECL performance of CuInZnS QDs, the concentration of H_2O_2, the pH value, and the scan rate were optimized as shown ESM Fig. S4. H_2O_2 worked as co-reactant in the ECL system. With the increase of the concentration of H_2O_2, the ECL intensity of CuInZnS QDs enhanced gradually. And the ECL intensity reached the maximum at 30 mmol/L H_2O_2 (ESM Fig. S4 (A)). The mechanism for the process of co-reactant ECL is according to the equations below:

$$H_2O_2 + e^- \rightarrow OH\cdot + OH^- \quad (4)$$

$$3OH\cdot \rightarrow H_2O + HO_2 \quad (5)$$

$$QD^-\cdot + OH\cdot \rightarrow QD^* + OH^- \quad (6)$$

$$QD^-\cdot + HO_2\cdot + OH^- \rightarrow QD^* + O_2 + H_2O \quad (7)$$

$$QD^* \rightarrow QD + h\nu \quad (8)$$

When the concentration of H_2O_2 increased, OH· produced by H_2O_2 ionization had disproportionation reaction and inhibit the ECL signal of CuInZnS QDs. The pH value also had an impact on ECL intensity of QDs. As shown in ESM Fig. S4 (B), the ECL signal reached the maximum at pH value 7.4. The scan rate determined the generation of excited QDs. When the scan rate was lower than 0.1 V/s, ECL intensity increased with the increase of the scan rate. When the scan rate was 0.1 V/s, the ECL signal reached the maximum (ESM Fig. S4 (C)).

Sensing mechanism

As shown in Fig. 2, the ECL intensity of CuInZnS QDs was ca. 300 in 0.1 mol/L phosphoric acid buffer and 2750 in 0.1 mol/L phosphoric acid buffer containing 30 mmol/L H_2O_2. The ECL intensity of QDs increased by 9 times when co-reactant (H_2O_2) was present in the system. And when the SOD was added in the system, because of the competition of HO_2, the ECL intensity of QDs was ca. 1250, which was suppressed by SOD. The sensing mechanism is as follows:

$$HO_2\cdot + OH^- \rightleftarrows O_2^-\cdot + H_2O \quad (9)$$

$$M^{(n+1)+}\text{–SOD} + O_2^-\cdot \rightarrow M^{n+}\text{–SOD} + O_2 \quad (10)$$

$$M^{n+}\text{–SOD} + O_2^-\cdot + 2H^+ \rightarrow M^{(n+1)+}\text{–SOD} + H_2O_2 \quad (11)$$

Equation (6) was the equilibrium of superoxide anion (OH^-) and superoxide ($HO_2\cdot$) in aqueous solution. Equations (10) and (11) were the process of SOD catalyzing the dismutation of superoxide anion radicals (O_2^-). When SOD

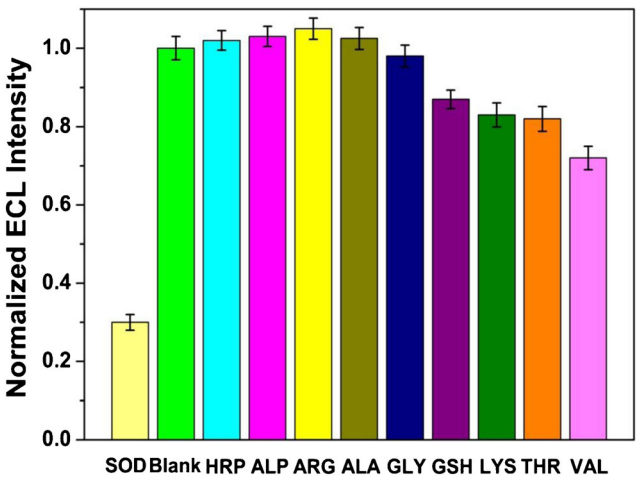

Fig. 5 The selectivity of the sensor. (0.5 μg/L enzymes (amino acids)/CuInZnS QDs in pH 7.4 0.1 mol/L phosphoric acid buffer containing 30 mmol L^{-1} H_2O_2)

Table 1 Results of determination of SOD in human serum samples

Sample	Spiked (nmol/L)	Founded (nmol/L)	Recovery (%)	RSD (%) ($n = 3$)
1	0.100	0.101	101.00	3.24
2	0.500	0.497	99.50	2.71
3	0.900	0.964	107.09	2.43

existed in the ECL sensing system, the competition resulted in the decrease of QD^* content in reaction (9) and finally quenched ECL signal.

Detection of the SOD

As shown in Fig. 3a and b, with the increasing of SOD concentration, the ECL signal decreased gradually. The linear equation between the concentration of SOD and ECL intensity was $I = -0.96\ C_{(SOD)} + 1.06$ with the correlation coefficient of 0.99. The limit of detection (LOD) was 0.03 μg/L. The stability of the proposed sensor was evaluated by successive measurements ($n = 11$) in phosphate buffer solution (pH = 7.4) containing 30 mmol/L H_2O_2 (Fig. 4a). The relative standard deviation (RSD) was 2.58%. It indicated that the outstanding stability of the sensor to detect SOD. In order to investigate the reproducibility of the sensor, the intra-assays and inter-assays were displayed in Fig. 4b. The relative standard deviations (ECL response) of intra- and inter-assays were 0.81% and 5.31%, respectively, which demonstrated an acceptable repeatability of the proposed sensor for the detection of SOD. The selectivity of the sensor was investigated by several amino acids and enzymes. The results were displayed in Fig. 5. An interference investigation was performed by using the solution containing 0.5 μg/L amino acids and enzymes. Compared with SOD, other enzymes had no quenching effect on CuInZnS QDs/H_2O_2 system. The interfere effect of amino acids were within the acceptable range. The applicability of the proposed ECL sensor was evaluated by detecting SOD in human serum with a standard addition method. As shown in Table 1, the range of recoveries was from 99.5 to 107.09% and the RSD was less than 3.24%.

The visual sensing

Furthermore, the ECL sensing process can be observed by smartphone camera. We also compared the exposure time during the photo taking process. The photos with the exposure time of 1 s were shown in ESM Fig. S5. We can see that under the same reaction conditions, the signal of the picture was far weak than the results in Fig. 6 (the exposure time of 3 s). In Fig. 6, CuInZnS QDs had a strong ECL emission and with a true-color ECL imaging strategy, we can observe the yellow ECL color of the QDs. After 0.5 μg/L SOD added in the system, the ECL signal became dark. When 1 μg/L SOD was added, the ECL signal was so weak that the CMOS sensor chip cannot catch the any signal. The above images can be converted into a thermal diagram through the algorithm, and

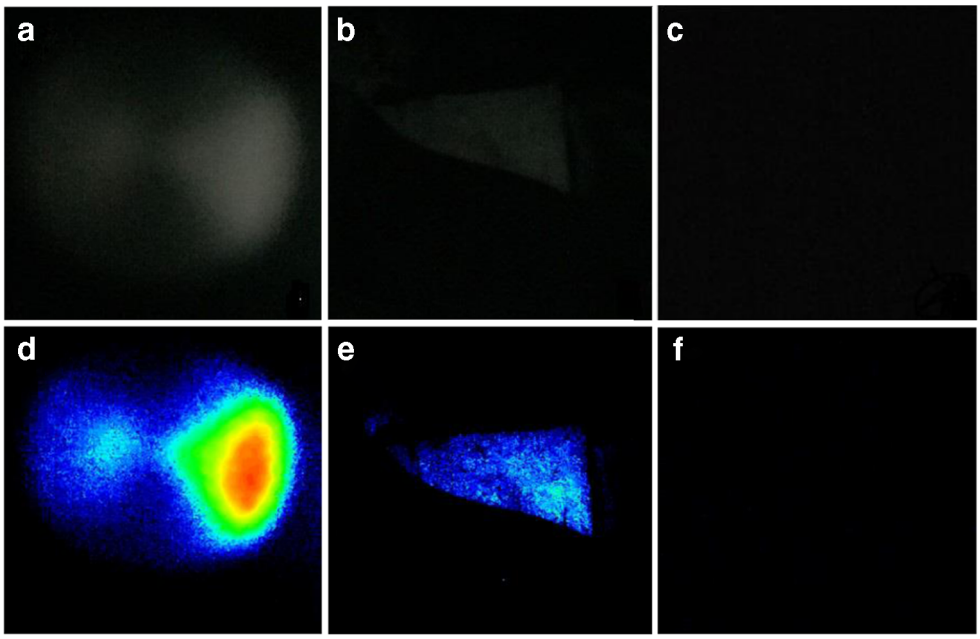

Fig. 6 Digital images of the ECL emission of **a** CuInZnS QDs, **b** 0.5 μg/L SOD/CuInZnS QDs, and **c** 1 μg/L SOD/CuInZnS QDs in pH 7.4 0.1 mol/L phosphoric acid buffer containing 30 mmol L^{-1} H_2O_2. The thermal map of the ECL emission of **d** CuInZnS QDs, **e** 0.5 μg/L SOD/CuInZnS QDs, and **f** 1 μg/L SOD/CuInZnS QDs in pH 7.4 0.1 mol/L phosphoric acid buffer containing 30 mmol L^{-1} H_2O_2 (The exposure time of 3 s)

the part with optical signal can be more directly and clearly distinguished. These results indicated the sensor had the potential to be used in clinical test.

Conclusion

A visual ECL sensing system was designed for detection of SOD by CuInZnS QDs. This work provided a novel visual ECL method of SOD detection. This new sensing mode improved the sensitivity and accuracy. Moreover, the ECL signal changes were recorded by the CMOS in the smartphone. These photos were further processed into thermal map for observing more intuitive. The strategy can be used for designing QD-based ECL sensors and visual detection instrument. This detection method has great application value in portable clinical detection.

Funding information This study received financial support from the National Natural Science Foundation of China (No 21005029), Youth Science Fund of Jilin Province (No 20140520081JH), and "Thirteenth Five Year" Project of the Science and Technology Research in the Education Department of Jilin Province, China (No JJKH20180125KJ).

Compliance with ethical standards

Statement on ethical approval The use of human serum samples in this study has been approved by the ethics committee of the China-Japan Union Hospital of Jilin University (No. 2019-NSFC-051).

Conflict of interest The authors declare that there are no conflicts of interest.

References

1. Nam S, Lee WY. Electrogenerated chemiluminescence of lucigenin at mesoporous platinum electrode and its biosensing application to superoxide dismutase. J Electroanal Chem. 2018;808:59–64.
2. Allen RG. Oxygen-reactive species and antioxidant responses during development: the metabolic paradox of cellular differentiation. Proc Soc Exp Biol Med. 1991;196:117–29.
3. Avraham KB, Schickler M, Sapoznikov D, Yarom R, Groner Y. Down's syndrome: abnormal neuromuscular junction in tongue of transgenic mice with elevated levels of human Cu/Zn-superoxide dismutase. Cell. 1988;54:823–9.
4. Groner Y, Elroy-Sterol OK, Avraham B, Schickler M, Knobler H, Minc-Golomb D, et al. Cell damage by excess CuZnSOD and Down's syndrome. Biomed Pharmacother. 1994;48:231–7.
5. Gu Q, Feng TN, Cao H, Tang YT, Ge X, Luo JD, et al. HIV-TAT mediated protein transduction of Cu/Zn-superoxide dismutase-1 (SOD1) protects skin cells from ionizing radiation. Radiat Oncol. 2013;8:253 (1–12).
6. Richter MM. Electrochemiluminescence (ECL). Chem Rev. 2004;104:3003–36.
7. Delaney J, Hogan CF, Tian JF, Shen W. Electrogenerated chemiluminescence detection in paper-based microfluidic sensors. Anal Chem. 2011;83(4):1300–6.
8. Jiang H, Ju HX. Electrochemiluminescence sensors for scavengers of hydroxyl radical based on its annihilation in CdSe quantum dots film/peroxide system. Anal Chem. 2007;79(17):6690–6.
9. Hu LZ, Xu GB. Applications and trends in electrochemiluminescence. Chem Soc Rev. 2010;39:3275–304.
10. Muzyka K. Current trends in the development of the electrochemiluminescent immunosensors. Biosens Bioelectron. 2014;54:393–407.
11. Deng SY, Lei JP, Huang Y, Cheng Y, Ju HX. Electrochemiluminescent quenching of quantum dots for ultrasensitive immunoassay through oxygen reduction catalyzed by nitrogen-doped graphene-supported hemin. Anal Chem. 2013;85(11):5390–6.
12. Carrajal MA, Ballesta-Claver J, Martinez-Olmos A, Captitan LF, Palna AJ. Portable system for photodiode-based electrochemiluminescence measurement with improved limit of detection. Sensors Actuators B Chem. 2015;221:956–61.
13. Ding ZF, Quinn BM, Haram SK, Pell LE, Korgel BA, Bard AJ. Electrochemistry and electrogenerated chemiluminescence from silicon nanocrystal quantum dots. Science. 2002;296(5571):1293–7.
14. Wang J, Shan Y, Zhao WW, Xu JJ, Chen HY. Gold nanoparticle enhanced electrochemiluminescence of CdS thin films for ultrasensitive thrombin detection. Anal Chem. 2011;83(11):4004–11.
15. Liu LL, Wang XY, Ma Q, Lin ZH, Chen SF, Li Y, et al. Multiplex electrochemiluminescence DNA sensor for determination of hepatitis B virus and hepatitis C virus based on multicolor quantum dots and au nanoparticles. Anal Chim Acta. 2016;916:92–101.
16. Le QL, Ding SN. Double signal amplification sandwich-structured immunosensor based on TiO_2 nanoparticles enhanced CdSe@ZnS QDs electrochemiluminescence and the dramatic quenching effect of Au@polydopamine nanoparticles. Sci Bull. 2016;61:931–8.
17. Liu SF, Zhang X, Yu YM, Zou GZ. A monochromatic electrochemiluminescence sensing strategy for dopamine with dual-stabilizers-capped CdSe quantum dots as emitters. Anal Chem. 2014;86(5):2784–8.
18. Chen XQ, Chen SF, Hu TY, Ma Q. Fluorescent aptasensor for adenosine based on the use of quaternary CuInZnS quantum dots and gold nanoparticles. Microchim Acta. 2017;184(5):1361–7.
19. Liu Y, Chen XQ, Ma Q. A novel amplified electrochemiluminescence biosensor based on au NPs@PDA@CuInZnS QDs nanocomposites for ultrasensitive detection of p53 gene. Biosens Bioelectron. 2018;117:240–5.
20. Chen XQ, Gui WY, Liu H, Ma Q. A novel CuZnInS quantum dot-based ECL sensing system for lysophosphatidic acid detection. Analyst. 2017;142:4142.
21. Chen XQ, Gui WY, Ma Q. Ultrasensitive detection of EGFR gene based on surface Plasmon resonance enhanced electrochemiluminescence of CuZnInS quantum dots. Anal Chim Acta. 2018;1009:73–80.
22. Bae YJ, Myung N, Bard AJ. Electrochemistry and electrogenerated chemiluminescence of CdTe nanoparticles. Nano Lett. 2004;4:1153–61.
23. Sun LF, Bao L, Hyun BR, Bartnik AC, Zhong YW, Reed JC, et al. Electrogenerated chemiluminescence from PbS quantum dots. Nano Lett. 2009;9(2):789–93.